Multiple Pion Production by Pions and the Isobar Model*†

V. P. KENNEY, J. G. DARDIS, AND G. BRUNHART
University of Kentucky, Lexington, Kentucky

(Received March 24, 1961; revised manuscript received August 23, 1961)

Multiple pion production by pions in hydrogen has been studied in the interaction $\pi^-+p\rightarrow p+\pi^-+\pi^++\pi^-$ at 810, 970, and 1100 Mev. Total cross sections were measured as 0.26±0.14 mb at 810 Mev, 0.32±0.21 mb at 970 Mev, and 0.54±0.32 mb at 1100 Mev. The kinematics of this pion production reaction at these energies appear to be reasonably well described by phase space dependence, but provide some support for an "isobar cascade" scheme in which the $T=\frac{1}{2}$ "second resonance" is excited and decays to the $T=J=\frac{3}{2}$ isobar, which decays in turn to a final state consisting of a nucleon, a recoil pion, and two decay pions.

I. INTRODUCTION

RECENT interpretations of the results of pion photoproduction experiments[1–8] and measurements of the pion scattering total cross section[9–10] suggest that in $\gamma-p$ and $\pi^{\pm}-p$ interactions the proton may be excited to resonant isobaric states such as are summarized in the hypothesized energy level scheme of Fig. 1.

There appear to be well-established isotopic spin-$\frac{1}{2}$ excitation levels at 600- and 890-Mev pion laboratory energies, with $d_{\frac{3}{2}}$ and $f_{\frac{5}{2}}$ L_J assignments based on recoil polarization measurements.[11] The possibility that there are $T=\frac{3}{2}$ isobaric levels at about 900 and 1330 Mev, has been pointed out by the Cornell Group[6,7] and discussed by Carruthers[6] and Peierls.[8]

The precise nature of the physical process responsible for the appearance of these resonant states is a matter of considerable discussion.[12,13] Presumably these effects are a consequence of either resonant pion-proton interactions, resonant pion-pion interactions, or some combination of these. Lindenbaum and Sternheimer[14] have suggested an extended isobar model of pion production by pions in which either the $T=J=\frac{3}{2}$ isobaric state $(I^*)_{\frac{3}{2}}$ or one of the higher $T=\frac{1}{2}$ levels $(I^*)_{\frac{1}{2}}$ is excited by the incident pion, the final state consisting of a recoil pion and a pion-nucleon pair originating in the decay of the isobar:

$$\pi+N\rightarrow(I^*)_{\frac{3}{2}}+\pi_2;\quad(I^*)_{\frac{3}{2}}\rightarrow N+\pi_1, \tag{1}$$

$$\pi+N\rightarrow(I^*)_{\frac{1}{2}}+\pi_3;\quad(I^*)_{\frac{1}{2}}\rightarrow N+\pi_4. \tag{2}$$

If the higher $T=\frac{1}{2}$ levels can be excited by pions, an alternative mode of decay of $(I^*)_{\frac{1}{2}}$ should be the isobar cascade process:

$$\pi+N\rightarrow(I^*)_{\frac{1}{2}}+\pi_3\rightarrow[(I^*)_{\frac{3}{2}}+\pi_5]+\pi_3\rightarrow(N+\pi_6)+\pi_5+\pi_3. \tag{3}$$

If the reaction (3) actually takes place, it should be expected to play a significant role in multiple pion production by pions in hydrogen. The reaction $\pi^-+p\rightarrow p+\pi^-+\pi^++\pi^-$, in which there are no neutral particles in the final state, provides an interesting experimental situation for an investigation to discover whether the isobar cascade decay scheme adequately explains the reaction kinematics.

The reaction was studied at 810, 970, and 1100-Mev incident pion laboratory kinetic energies. At the lowest energy, the total energy in the center-of-mass system is 1640 Mev, which is below the peak for excitation of the

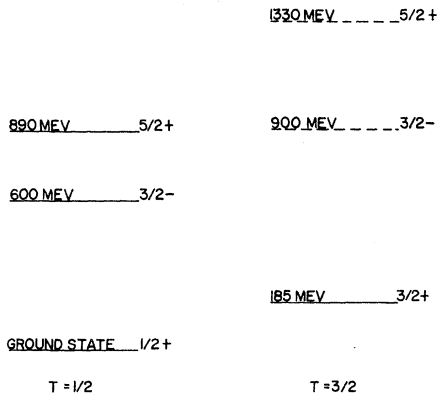

FIG. 1. Resonant pion-proton isobaric states, with excitation energies referred to the laboratory system of the incoming pion. The comparatively well-established $T=J=\frac{3}{2}$ level and the two $T=\frac{1}{2}$ levels are shown as solid lines, with the hypothesized higher excited $T=\frac{3}{2}$ shown as dashed lines.

* Supported in part by the National Science Foundation.

† Experiment carried out in cooperation with the Alvarez bubble chamber group of the Lawrence Radiation Laboratory.

[1] R. F. Peierls, Phys. Rev. Letters **1**, 174 (1958).
[2] J. J. Sakurai, Phys. Rev. Letters **1**, 258 (1958).
[3] M. Moravcsik, Phys. Rev. Letters **2**, 171 (1959).
[4] P. C. Stein, Phys. Rev. Letters **2**, 473 (1959).
[5] L. F. Landovitz and L. Marshall, Phys. Rev. Letters **3**, 190 (1959); **4**, 474 (1960).
[6] P. Carruthers, Phys. Rev. Letters **4**, 303 (1960); Phys. Rev. Letters **6**, 567 (1961).
[7] P. Carruthers and H. Bethe, Phys. Rev. Letters, **4**, 536 (1960).
[8] R. F. Peierls, Phys. Rev. Letters **5**, 166 (1960); Phys. Rev. **118**, 325 (1960).
[9] T. J. Devlin, B. C. Barish, W. N. Hess, V. Perez-Mendez, and J. Solomon, Phys. Rev. Letters **4**, 242 (1960).
[10] J. C. Brisson, J. Detoef, P. Falk-Vairant, and L. van Rossum, Phys. Rev. Letters **3**, 561 (1959); P. Falk-Vairant and G. Valladas, *Proceedings of the 1960 Annual International Conference on High-Energy Physics at Rochester* (Interscience Publishers, Inc., New York, 1960), p. 38.
[11] G. Salvini, *Proceedings of the 1960 Annual International Conference on High-Energy Physics at Rochester* (Interscience Publishers, Inc., New York, 1960), p. 3.
[12] I. Derado, Nuovo cimento **15**, 853 (1960).
[13] R. M. Sternheimer and S. J. Lindenbaum, Phys. Rev. **109**, 1723 (1958).
[14] S. J. Lindenbaum and R. M. Sternheimer, Phys. Rev. Letters **5**, 24 (1960); R. M. Sternheimer and S. J. Lindenbaum, Phys. Rev. **123**, 333 (1961).

lowest $T=\frac{1}{2}$ level, assuming an excitation energy of 600 Mev in the laboratory system for that state. At 970 and 1100 Mev there is sufficient energy to reach the lower $T=\frac{1}{2}$ level, but excitation of the 890-Mev isobaric state is unlikely. Consequently, one might hope to contrast the reactions observed at 810 Mev with those carried out at the higher energies to observe the effect on double pion production of the lower $T=\frac{1}{2}$ isobaric state.

II. PROCEDURE

Bubble chamber film from the Lawrence Radiation Laboratory 10-in. hydrogen bubble chamber was made available by the Alvarez group. Four-prong events characteristic of the $\pi^-+p\rightarrow p+\pi^-+\pi^++\pi^-$ reaction, which are quite striking in appearance, were noted with high efficiency by scanners examining film in the study of strange particle associated production, described in detail elsewhere.[15] Contact prints were made of film frames on which four-prong events were recorded, and fiducial-mark measurements on prints and originals were compared under microscope to insure that no distortion was introduced in the process.

Measurements of track curvature and projected track direction in each stereo view were made on a projection table using a scale and templates on which were ruled curves of known radius. The stereoscopic reconstruction and subsequent calculations were carried out on an IBM-650 computer.

The precision of the track curvature measurements was a function of the degree of curvature and the length of the tracks measured. The direction cosines were computed from measurements of coordinate points in each stereo view, reconstructed in space, and depended in accuracy on the relative orientation of the points with respect to the axis of the two stereo lenses.

Some error was introduced into the measurements by turbulent distortion of the tracks in the liquid, an appreciable factor in some regions of the chamber.[16]

In order to gain some idea of the combined errors of momentum and angle measurement, including distortion, the total momentum imbalance vector in each plane of projection was computed from momentum conservation for each event:

$$\alpha=p_{\text{in}}-\sum p_i\cos\theta_i, \tag{3}$$

$$\beta=\sum p_i\sin\theta_i\cos\phi_i, \tag{4}$$

$$\gamma=\sum p_i\sin\theta_i\sin\phi_i, \tag{5}$$

where p_{in} is the assumed nominal incoming momentum and p_i, θ_i and ϕ_i are the measured momenta and space angles of each of four outgoing tracks in each event.

[15] F. Crawford, M. Cresti, M. L. Good, K. Gottstein, E. Lyman, F. Solmitz, L. Stevenson, and H. Ticho, Phys. Rev. **108**, 1102 (1957); *1958 Annual International Conference on High-Energy Physics at CERN* (CERN Scientific Information Service, Geneva, 1958), p. 323.

[16] M. Cresti, University of California Lawrence Radiation Laboratory internal report (unpublished), Berkeley, California.

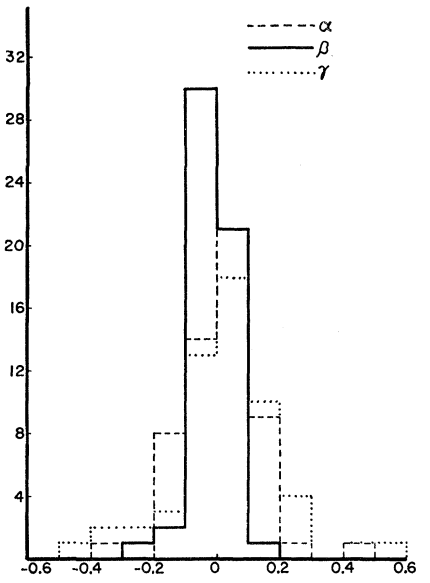

FIG. 2. Distributions of momentum imbalance vectors in each of 3 mutally perpendicular directions calculated for events at 810 Mev.

The distributions of the momentum imbalance vectors α, β, and γ for the identified events at 810 Mev is shown in Fig. 2. From the mean values $\bar{\alpha}$, $\bar{\beta}$, and $\bar{\gamma}$ one can compute a percent total momentum imbalance

$$\tau=100(\bar{\alpha}^2+\bar{\beta}^2+\bar{\gamma}^2)^{\frac{1}{2}}/p_{\text{in}}. \tag{6}$$

At 810 Mev, where $\bar{\alpha}=0.106$ Bev/c, $\bar{\beta}=0.055$ Bev/c, and $\bar{\gamma}=0.155$ Bev/c, the value of τ was 21%, and represents a measure of the combined average momentum error for the four outgoing tracks in each event. The momentum imbalance distributions at 970 and 1100 Mev were comparable.

The only four-prong events for which one would expect the visible tracks to conserve momentum were

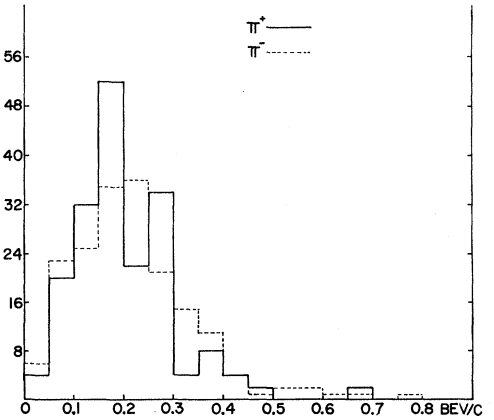

FIG. 3. Momentum distributions in the center of mass for positive and negative pions from the reaction $\pi^-+p\rightarrow p+\pi^-+\pi^++\pi^-$ at 1100 Mev compared. The π^+ distribution is normalized to the number of negative pions.

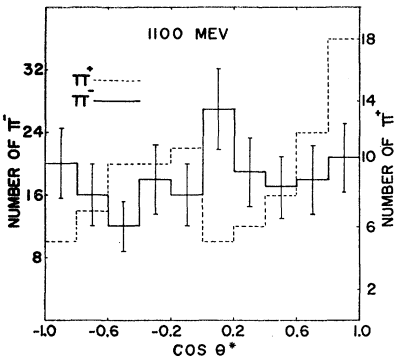

FIG. 4. Scattering angle distributions in the center of mass for positive and negative pions at 1100 Mev compared.

the events of type $\pi^-+p\rightarrow p+\pi^++\pi^-+\pi^-$. Event selection was made from the calculated values of the momentum imbalance α, β, and γ, using Chauvenet's criterion[17] to reject those events whose momentum imbalance values deviated from the mean values by amounts such that their probability of occurrence would be $\leq 1/2n$, where n was the total number of events. The principal background was from events in which neutral pions were produced, with one of the decay photons converting internally (Dalitz decay) to provide two additional prongs at the interaction point. These events were readily identified from the ionization density and curvature of the electron-positron pair, as well as from momentum imbalance considerations. The events so identified were selected as part of a separate study of neutral pion production by pions.[18] A total of 55 events were identified as $p+\pi^-+\pi^++\pi^-$ at 810 Mev, 70 at 970 Mev, and 92 at 1100 Mev, for a total of 217 events in all.

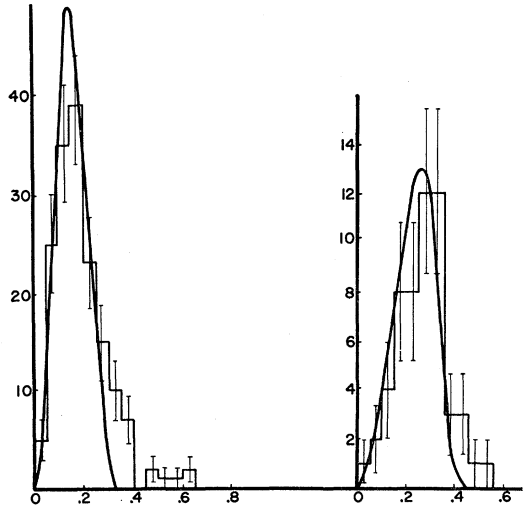

FIG. 5. Center-of-mass momentum distributions for all pions (left) and for protons (right) at 810 Mev. Solid curves are distributions computed from four-body phase space calculations.

[17] A. G. Worthing and J. Geffner, *Treatment of Experimental Data* (John Wiley & Sons, Inc., New York, 1943), p. 170.
[18] C. D. Gall, W. D. Shephard, and V. P. Kenney (to be published).

In view of the difficulty of properly weighting the momentum imbalance contributions of each track, particularly in those events in which turbulent distortion was appreciable, no attempt was made to fit individual events to the incoming particle energy and the requirements of energy-momentum conservation; the results which follow are presented in terms of directly measured quantities in each instance.

III. RESULTS

The parameters computed for the selected $p+\pi^-+\pi^++\pi^-$ events at each of the three incoming pion energies were the center-of-mass momentum of each of the outgoing particles, p^*, the center-of-mass scattering angle, θ^*, the angle Ψ^* between outgoing pairs of particles in the center-of-mass system, and the Q values for pairs of outgoing particles. The value $Q=[(E^*)^2-(p^*)^2]^{\frac{1}{2}}-(M_1+M_2)$, the difference in mass-energy of the hypothesized intermediate two-body state or isobar and the rest energies of the final-state particles, was calculated for possible $\pi-\pi$ as well as $\pi-p$ intermediate states.

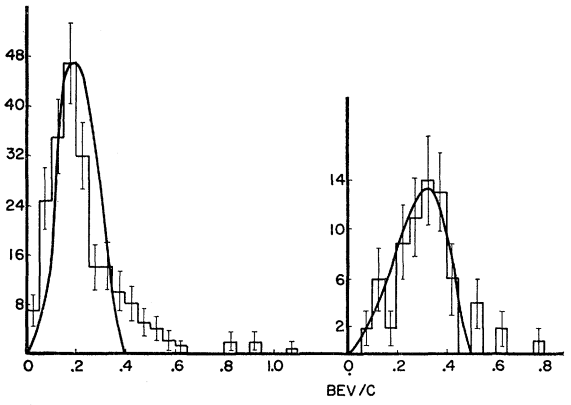

FIG. 6. Center-of-mass momentum distributions for all pions (left) and for protons (right) at 970 Mev. Solid curves are distributions computed from four-body phase space calculations.

Momentum distributions were the same, within statistics, for outgoing positive and negative pions at each of the three incoming pion energies, as shown for the reaction at 1100 Mev in Fig. 3. In the same way there appeared to be no appreciable difference in the scattering angle θ^* of positive and negative pions, as shown for the 1100-Mev reaction in Fig. 4, nor was there any appreciable difference in the distributions of the correlation angle Ψ^* for particle pairs involving positive and negative pions. As a consequence positive and negative pions were considered together in the distributions of p^*, $\cos\theta^*$, and $\cos\Psi^*$ presented below.

The momentum distributions for all pions and for the protons from the double-pion production reaction are shown in Figs. 5–7 for incoming laboratory-system pion

energies of 810, 970, and 1100 Mev. The pion momenta appear to peak at about 200 Mev/c at each of the three energies considered, while the peak proton momentum increases from a value of 230 Mev/c for the 810-Mev events to a value of 320 Mev/c for the 1100-Mev events. Momentum distributions computed from the covariant phase space program of Hoang and Young[19] are plotted for comparison.

The scattering angle distributions for all pions and for protons at each incoming energy are shown in Fig. 8. The nucleons are scattered predominantly into the backward hemisphere, very strongly so at the two higher energies. The pion distribution at all three energies is very nearly isotropic.

Distributions of the angle between emitted particle pairs are shown for both pion-pion and pion-proton pairs in Figs. 9–11; distributions computed from phase space factors[18] alone are presented for comparison. The opening angle between pion-proton pairs tends to be large at all energies. The angle between pion-pion pairs

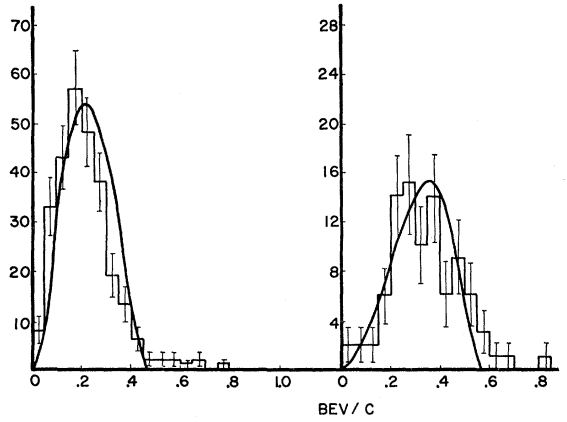

FIG. 7. Center-of-mass momentum distributions for all pions (left) and for protons (right) at 1100 Mev. Solid curves are distributions computed from four-body phase space calculations.

shifts gradually toward larger angles with increasing incoming pion energy.

Distributions of Q values for (π^-,p) and (π^+,p) pairs at each of the three energies are shown in Fig. 12. Both (π^-,p) and (π^+,p) distributions show a similar appearance at 810 Mev, peaking at low Q values. At the two higher energies the (π^-,p) and (π^+,p) Q distributions look somewhat different, the (π^+,p) Q values being considerably more concentrated at the lower energies than the (π^-,p), although the peaks remain at approximately the same Q-value energy. The Q-value distributions for pion-pion pairs shown in Fig. 13 would seem to indicate that there is little difference between (π^+,π^-) Q values and (π^-,π^-) Q values at any of the three incident energies.

A calculation of the total cross section for the $\pi^-+p\rightarrow$

[19] T. H. Hoang and J. Young, University of California Lawrence Radiation Laboratory Report UCRL-9050, 1960 (unpublished) Berkeley, California.

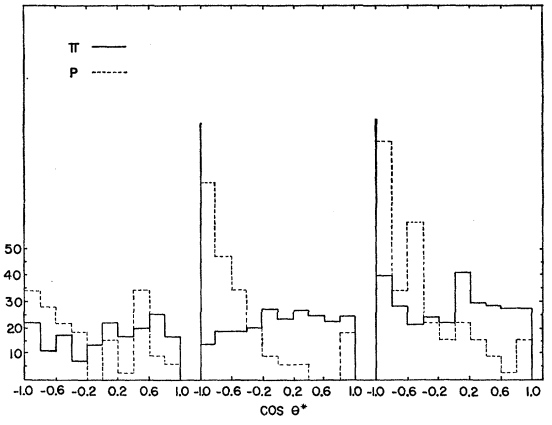

FIG. 8. Center-of-mass scattering angle distributions for all pion and for protons for events at 810 (left), 970 (center), and 1100 Mev (right). The proton distribution is normalized to the number of pions.

$p+\pi^-+\pi^++\pi^-$ reaction was made for each of the three energies studied. The total pion path length γ through a fiducial volume in the central portion of the chamber was determined from the expression

$$\gamma=(L)(M)(N_1)(C_1)(C_2), \tag{7}$$

where L is the total visible track length measured in each frame in which an event was identified and which contained no more than 40 tracks, M the demagnification factor to chamber dimensions, N_1 the total number of frames in the sample studied, C_1 a correction factor for the excess in the number of tracks contained in the frames in which identified events occurred (measured to be 14%), and C_2 the correction for the number of frames with less than one or more than 40 tracks. The cross sections were then determined from the relation:

$$\sigma=N_2/(3.49\times10^{22})\gamma \text{ cm}^{-2}, \tag{8}$$

where N_2 is the total number of events found within the fiducial volume of frames which contained no more than

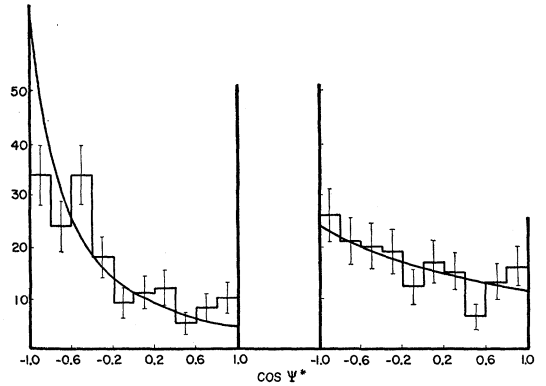

FIG. 9. Distribution of angles between particles for all pion-proton pairs (left) and pion-pion pairs (right) in the center of mass for events at 810 Mev. Curves are computed from four-body phase space calculations.

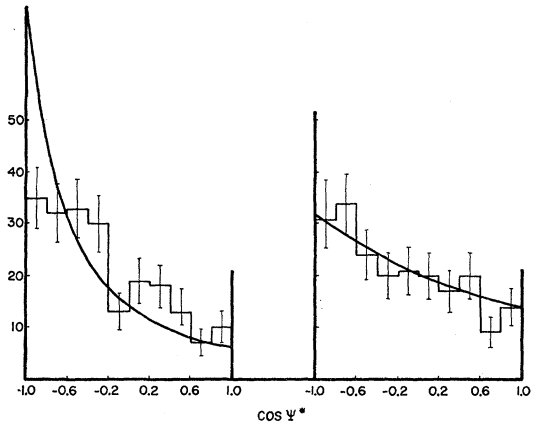

FIG. 10. Distribution of angles between particles for all pion-proton pairs (left) and pion-pion pairs (right) in the center-of-mass for events at 970 Mev. Solid curves are computed from four-body phase space calculations.

40 tracks, and the numerical factor is the product of the density of liquid hydrogen under the conditions of this experiment and the ratio of Avogadro's number to the atomic weight of hydrogen.

The scanning efficiency for finding these four-prong events was assumed to be $\approx 100\%$. The total cross-section values were then found to be 0.26 ± 0.14 mb at 810 Mev, 0.32 ± 0.21 mb at 970 Mev, and 0.54 ± 0.32 mb at 1100 Mev. The errors given are the statistical errors which include the propagated errors determined for each term in Eq. (7).

IV. DISCUSSION

The most notable feature of the reaction studied is the relative lack of difference in behavior of positive and negative pions, as revealed by measurements of momentum, scattering angle, correlation angle, and Q value. This contrasts strongly with the situation in the single-pion production reactions:

$$\pi^-+p \rightarrow p+\pi^-+\pi^0 \tag{9}$$

$$\rightarrow n+\pi^++\pi^-, \tag{10}$$

studied by various authors,[20] and the photoproduction reaction,

$$\gamma+p \rightarrow p+\pi^++\pi^-, \tag{11}$$

studied by the Cornell group.[21] This behavior, together with the rather good agreement of the distributions of Figs. 5–7 and 9–11 computed from phase space, suggests that multiple pion production, in contrast with single pion production, may be described rather well in terms of a simple statistical model.

At the same time the isobar cascade model for multiple pion production predicts momentum distributions for the final-state particles which are also in good agreement with the measured values. In Fig. 14 the predictions of the isobar model[22] and the phase space calculation are contrasted for both the proton and the positive pion at 1100 Mev, and it seems clear that both theoretical curves are consistent with the experimental data, within statistics. On the isobar model all three pion momenta are expected to peak in the region of ≈ 200 Mev/c at each of the energies considered, and the

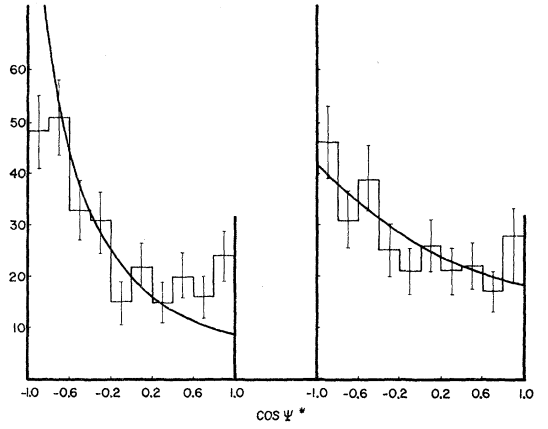

FIG. 11. Distributions of angles between particles for all pion-proton pairs (left) and pion-pion pairs (right) in the center-of-mass for events at 1100 Mev. Solid curves are computed from four-body phase space calculations.

failure of the positive and negative pions to show appreciable kinematic differences could be explained accordingly.

In order to investigate whether the hypothesized isobar cascade process [Eq. (3)], does indeed take place, one must attempt to distinguish the recoil pion π_3 from the isobar decay pions π_5 and π_6. From isotopic spin considerations, one would expect the $(I^*)_{\frac{3}{2}}$ isobar decay to favor production of a (π^+,p) pair. Sternheimer[22] estimates that the π_6 decay pion will be positive and the remaining pions π_3 and π_5 negative in approximately 90% of all cases. Differences in the relative $(\pi^\pm,p)$ Q values and in the nucleon angular distributions at 810 Mev compared to 970 and 1100 Mev may suggest that some such process is important, inasmuch as reactions at the lowest energy take place below the peak energy for producing the heavier $(I^*)_{\frac{3}{2}}$ isobar and an additional pion, whereas the reactions at 970 and 1100 Mev are well above the energy corresponding to the resonance peak. At 810 Mev, where the isobar cascade mode of reaction is unlikely, the Q distributions for (π^+,p) and for (π^-,p) pairs have much the same form (Fig. 12). The ratio of events with $Q>200$ Mev: $Q<200$ Mev is

[20] W. D. Walker, F. Hushfar, and W. D. Shephard, Phys. Rev. **104**, 527 (1956); J. G. Dardis and V. P. Kenney, Bull. Am. Phys. Soc. **4**, 266 (1959); I. Derado and N. Schmitz, Phys. Rev. **118**, 309 (1960); V. Alles-Borelli, S. Bergia, E. Perea Ferreira, and P. Waloschek, Nuovo cimento **14**, 211 (1959); E. Pickup, F. Ayer, and E. O. Salant, Phys. Rev. Letters **5**, 161 (1960).

[21] B. M. Chasan, G. Cocconi, V. T. Cocconi, R. M. Schectman, and D. H. White, Phys. Rev. **119**, 811 (1960).

[22] R. M. Sternheimer (private communication).

0.17 ± 0.06 for the (π^+,p) pairs and 0.15 ± 0.04 for the (π^-,p) pairs. At 970 Mev the same ratio is 0.06 ± 0.03 for the (π^+,p) pairs, consistent within statistics with the 810-Mev ratio, while for the (π^-,p) pairs the ratio is 0.41 ± 0.08, considerably higher. At 1100 Mev the (π^+,p) ratio is 0.12 ± 14, again consistent with the 810-Mev ratio, while the (π^-,p) pair ratio is 0.36 ± 0.06. The statistics are largely limited by the small number of events above 200 Mev/c in each case.

One might associate the apparent constancy of (π^+,p) Q values, and spreading of (π^-,p) Q values with increasing energy, with the predictions of the isobar cascade model, in which the (π^+,p) pair is identified with the $(I^*)_{\frac{3}{3}}$ decay Q value of 145 Mev. By similar reasoning, if the backward peaking of the proton observed at 810 Mev in Fig. 7 is associated with an intermediate step in which a comparatively massive $(I^*)_{\frac{3}{3}}$ is frequently formed together with two pions, one might then expect that at higher energies, where the final proton might arise from a two-step process involving successive decay of two massive isobars, the backward peaking of the proton would be more pronounced. In Fig. 7 the ratio of protons scattered backward: forward increases significantly from a value 1.5 ± 0.4 at 810 Mev to values 6.0 ± 2.4 at 970 Mev and 3.3 ± 0.8 at 1100 Mev.

It should be pointed out, nonetheless, that the (π^+,p)

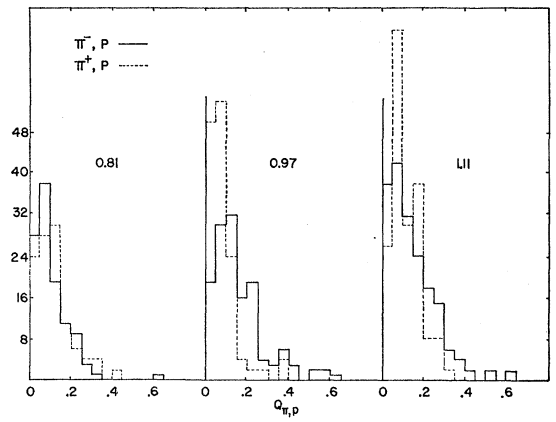

FIG. 12. Distributions of (π^-,p) and (π^+,p) Q values for events at 810, 970, and 1100 Mev. The (π^+,p) distribution is normalized to the number of (π^-,p) pairs.

Q values seem actually to peak below the nominal $(I^*)_{\frac{3}{3}}$ value for events at 970 and 1100 Mev, and that the peak (π^-,p) Q value does not shift appreciably with energy. The statistics throughout are very limited, and the error propagated in the Q calculation is appreciable. The increase in the backward peaking of the protons at energies above 810 Mev could have a variety of kinematic explanations. Indeed, the data seem more suggestive that some sort of difference in interaction kinematics exists at 810 Mev compared to higher energies, than indicative of the origin of this effect.

An alternative approach for multiple pion production by pions is the possibility that pion production may take place in the rescattering of pions from a primary pion-pion interaction, or that pion-pion and pion-nucleon resonant interactions may both take place, with pion production proceeding through both branches,[23] as shown in Fig. 15. The observed strong backward peaking of the recoil nucleon would be consistent with such a picture.

If the incoming π^- interacts with a negative pion, the pion-pion state will have isotopic spin $T=2$, and outgoing pions one, two, and three in Fig. 15 will be π^-, π^-, and π^+, respectively. If the incoming pion interacts with a positive pion, the intermediate pion-pion interaction will be an isotopic spin mixture of $T=0$, 1, 2 states, and outgoing pions one, two, and three will be π^-, π^+, and π^-, respectively. Strong peaking in the Q distribution of the (π_1,π_2) pair might indicate that a reaction of this type was taking place; the problem, of course, is to distinguish this pair from the (π_1,π_3) and (π_2,π_3) pairs. Only in the isotopic spin $T=2$ interaction, where π_1 and π_2 are both negative, is the identification unambiguous.

From the (π,π) pair histograms of Fig. 13 it would appear that both (π^-,π^-) and (π^-,π^+) pairs have very similar Q distributions, the widths of which become proportionately wider with increasing energy. It is probably not possible to rule out the significance of a pion-pion contribution to the multiple pion production reaction on this account, however, and the strong $T=J=\frac{3}{2}$ reaction discussed above should be evident in either case.

In summary, it would appear that most of the kinematic characteristics of the reaction, $\pi^-+p\rightarrow p+\pi^-+\pi^++\pi^-$, at the energies studied are reasonably well described by a simple phase space dependence, within the limits of accuracy of the measurements. Some support for an isobar cascade model in which a heavy

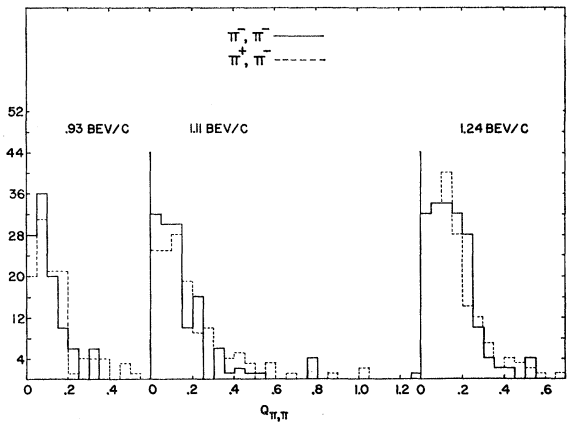

FIG. 13. Distributions of (π^-,π^-) and (π^+,π^-) Q values for events at 810 (left), 970 (center), and 1100 Mev (right). The (π^-,π^-) distribution is normalized to the number of (π^+,π^-) pairs.

[23] F. Salzman and G. Salzman, Phys. Rev. **120**, 599 (1960); S. D. Drell and F. Zachariasen, Phys. Rev. Letters **5**, 66 (1960); A. Erwin (private communication).

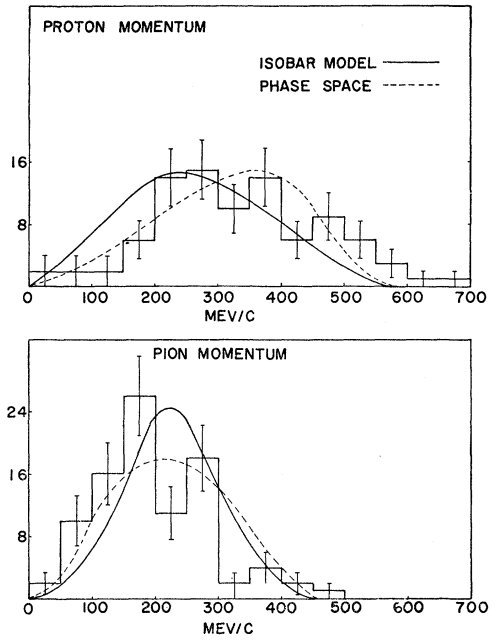

FIG. 14. Comparison of cascade isobar model and phase space momentum distributions with experimental values for protons (top) and positive pions (bottom) at 1100 Mev.

$(I^*)_{\frac{1}{2}}$ decays by pion emission to a $(I^*)_{\frac{3}{2}}$ isobar, and then to a final-state nucleon, is suggested by differences in the nucleon angle distribution and $(\pi^{\pm},p)$ Q values at 810 Mev compared to the higher energies, at which the energy availability would be more favorable to this process. These effects are not, however, very striking, and their explanation in terms of an isobar decay cascade is not unambiguous. Pion production mechanisms initiated by a pion-pion interaction in particular cannot be ruled out.

Inasmuch as experimental uncertainties do not permit an unambiguous determination of the reaction

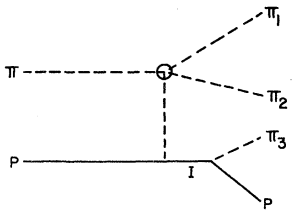

FIG. 15. Diagram for pion production through simultaneous pion-pion and pion-proton resonant interaction. Pions one and two are produced in the (π,π) interaction and pion three is the decay pion from the (π,p) isobar I.

mechanism, it would be of interest to repeat these measurements with improved statistics at an energy sufficiently high that the predictions of phase space dependence and the isobar model differ more appreciably than in the present experiment. It should be noted, however, that at very much higher energies the higher mass isobaric states may be expected to make a contribution and the analysis may consequently be more complicated.

ACKNOWLEDGMENTS

The authors wish to express their appreciation to Dr. Luis Alvarez and his coworkers at the University of California Lawrence Radiation Laboratory for making the 10-in. bubble chamber data available for study. Discussions with Dr. H. Bradner and Dr. F. Crawford were particularly helpful in the early stages of this work. We wish to thank Dr. R. Sternheimer for his assistance in applying the extended isobar model to the present data, and for making available the results of his and Dr. S. J. Lindenbaum's calculations prior to publication.

This work owes a great deal to the interest and many suggestions of Dr. W. B. Fowler, and to discussions with Dr. W. D. Shephard.

Particular thanks are due to R. G. West for accurately reproducing selected frames of bubble chamber photographs, and to Ron Cummings and the University of Kentucky Computing Center for assistance in the data analysis.